Proceedings of Ninth World Conference on Earthquake Engineering
August 2-9, 1988, Tokyo-Kyoto, JAPAN (Vol.VI)

10-4-16

SEISMIC OBSERVATION AND ANALYSIS OF UNDERGROUND CRUDE OIL STORAGE FACILITY

Naonobu TAKEWAKI[1], Takashi YOSHIMURA[1], Kenji AOKI[2],
Tetsuya HANAMURA[3] and Takaya TAJIMA[4]

[1]Shimizu Corporation, Chiyoda-ku, Tokyo, Japan
[2]Kajima Corporation, Minato-ku, Tokyo, Japan
[3]Taisei Corporation, Shinjuku-ku, Tokyo, Japan
[4]JGC Corporation, Chiyoda-ku, Tokyo, Japan

SUMMARY

In this paper, the earthquake records observed at an underground crude oil storage facility in the rock ground are presented along with their spectral characteristics, and the observed strain records are simulated by an analytical method based on the study by Mow and Mente. As the result of analyses, it is found that the existence of the underground storage cavern does not have much influence on the earthquake motion in the rock ground. Furthermore, it is concluded that the dynamic stress around the storage cavern during earthquakes can be estimated by this simple analytical method.

INTRODUCTION

The underground petroleum storage facility has a history of several decades in Europe and North America. In order to investigate its applicability in JAPAN where the geological structure is rather complex, a demonstration plant was constructed in 1981 by Japan National Oil Corporation (Ref. 1). The plant has a horizontal-water-curtain-type underground crude oil storage tank of 25,000 kl capacity. The earthquake observation has been carried out in the rock ground surrounding the underground storage cavern as well as the investigation on geomechanics and hydraulics (Ref. 2).

In this paper, we present the dynamic characteristics of the storage cavern and its surrounding rock ground evaluated from the observed earthquake records and the deformation of the service tunnel during earthquakes. Also, the analytical method is employed when estimating the dynamic stress around a cavern based on the observed records.

OUTLINE OF THE EARTHQUAKE OBSERVATION

The demonstration plant is located in Kikuma, Shikoku Island in Japan as shown in Fig. 1. This area mostly consists of granitic rocks and has no major faults and fracture zones. The result of the elastic wave exploration at the bore hole in the site is shown in Table 1. The rock from the surface to about EL -5 m is weathered and the deeper rock is fresh.

The demonstration plant comprises a storage cavern for crude oil with supplementary facilities such as service tunnels, a water tunnel, a dry pump room, vertical shafts and access tunnels for the construction work as shown in

Fig. 2. The storage cavern is 15 m wide, 20 m high and 112 m long and located at the depth between EL -42 m and -62 m.

The location of the accelerometers are shown in Fig. 3. The acceleration is measured on the ground surface (A-1), in the service tunnel within the weathered stratum (A-6, A-7), on the bottom of the storage cavern (A-8), in the rock at the depths similar to A-8 (A-2, A-4, A-5), and in the deepest rock (A-3). The location of the strain gauges are shown in Fig. 4. Fourteen strain gauges are installed at two cross sections of the service tunnel. The strain gauges given in parentheses in Fig. 4 (S-4, S-8, S-11, S-14) are installed in the longitudinal direction and the others in the transverse direction. The earthquake observation was started in December 1981 and 34 earthquakes were observed up to January 1988.

ANALYSIS OF THE OBSERVED RECORDS

Acceleration Records Figure 5 shows the distribution of the maximum acceleration ratio in the vertical direction (A-1, A-6, A-2 and A-3). The similar distribution in the horizontal direction is also shown (A-2, A-4, A-5 and A-8). These points are located at a similar depth. In the figure, the lines are drawn for the horizontal components of the 8 observed earthquakes whose maximum values at A-3 were lager than 1.0 gal. It is observed that the maximum acceleration ratios of the earthquakes in the vertical direction slightly change in the fresh rock. However, the motions are amplified drastically as they approach the weathered stratum near the ground surface. The variation of the ratios at A-2, A-4, A-5 and A-8 is very small. As a result, there is only a little difference in the motions of the fresh rock at a similar depth and the motions are not substantially influenced by the existence of the storage cavern.

Figure 6 shows the average Fourier spectra for the N-S component of the above 8 earthquakes. Here the maximum acceleration of these earthquakes is normalized to 1.0 so that their Fourier spectra can be averaged. The features of the spectra at A-2, A-4, A-5 and A-8 in the fresh rock are in good conformity and they also look similar to that at the deepest point A-3. In addition to these, the maximum values and the phases exhibit a good correspondence with one another for the observed acceleration waves at A-2, A-3, A-4, A-5 and A-8, although the figures for them are not shown here. As described above, the dynamic characteristics at A-8 on the bottom of the storage cavern correspond to that at the other points in the fresh rock. Therefore, the existence of the storage cavern does not have much influence on the earthquake motion in the fresh rock.

The predominant frequencies at A-1 on the ground surface are about 6 Hz and 9 Hz. Since these frequencies are not predominant at the other points, it seems that they are the predominant frequencies of the near-surface ground.

Strain Records Table 2 shows the maximum strain values of the 6 earthquakes in which the strain was recorded at all the observation points. As is evident from Table 2, the maximum strain values are almost equal between the symmetrical points on the side wall of the service tunnel (S-1 and S-6, and S-7 and S-13). The maximum values at the points of the arch (S-2, S-5, S-9 and S-12) are about one to three times larger than those at the points on the side wall. It is also found that the maximum values in the longitudinal direction (S-4, S-8, S-11 and S-14) are about 1/10 to 1/3 of those in the transverse direction.

Figure 7 shows the power spectra of the strain at S-1 to S-6 for the No.22 earthquake. The predominant frequencies at the symmetrical points on the side wall (S-1 and S-6) are about 5.5 Hz and 6 Hz, and they exhibit a good agreement

with each other. The shapes of the power spectra of S-2, S-3 and S-5, which are the horizontal observation points and the symmetrical points of the arch, exhibit a good correspondence with one another and their predominant frequency is about 5 Hz. Though the B-B cross section and the C-C cross section differ in the dimension and the direction, the features of the power spectra of the corresponding points are quite similar for these two cross sections (the figures for which are omitted in this paper). It is considered that these results are caused by the predominant frequency of the weathered stratum near the ground surface.

In order to examine the phase characteristics of the strain records, the frequency contents of 4.0 to 7.0 Hz of the observed records during the No.22 earthquake are filtered out and their maximum values are normalized to 1.0. Such filtered principal motions are shown in Fig. 8 where those of the symmetrical points are drawn on the same axis. As is evident from this figure, the phases of the strain at S-1 and S-6, and S-7 and S-13 on the side wall, which are the vertical components, are in good agreement. However, the strain at S-2 and S-5, and S-9 and S-12 of the arch, which comprise the horizontal component and the vertical component, are completely in the opposite phase. Although the deformation of the service tunnel during earthquakes is composed of the various modes, its deformation can be decomposed into two dominant modes which are the uniform expansion and contraction type mode in the vertical direction and the shearing type mode in the horizontal direction.

SIMULATION BY THE ANALYTICAL METHOD

Analytical method Mow and Mente (Ref. 3) investigated the dynamic stress and the strain around a cylindrical discontinuity in an infinite elastic medium subjected to a plane harmonic shear wave as shown in Fig. 9. In this paper, employing this method, the simulation of the observed strain records around the service tunnel is carried out using the No.22 earthquake. At that time, the input acceleration is decomposed into the harmonic waves with the aid of the fast Fourier transform and they are used for the incident shear waves.

The service tunnel in which the strain gauges are installed is in the weathered stratum. Therefore, the incident motion to the weathered stratum is estimated from the observed acceleration at the deepest point A-3 using the computer code SHAKE. The maximum value of the incident acceleration is 0.59 gal. The rock properties of the weathered stratum from the ground surface to EL ±0 m are not obtained in the elastic wave exploration and they are assumed to be the same values as those of the weathered stratum from EL ±0 m to -4.98 m. The service tunnel is assumed to be a cylindrical cavern with the diameter 4.5 m in an infinite elastic medium.

Results of the analysis Figure 10 shows the strain waves and their Fourier spectra at S-2 of which the observed maximum value is the largest in the B-B cross section. Though it is assumed that the service tunnel is a cylindrical cavern in an infinite elastic medium subject to the incident plane shear wave, the maximum strain and its predominant frequency obtained by the analysis exhibit a good agreement with those by the observation. Considering these results, the strain around the service tunnel can be well simulated by this analytical method. In other words, it is considered that the deformation of the service tunnel during earthquakes is dominated by the shearing type mode.

ESTIMATION OF THE DYNAMIC STRESS AROUND THE LARGE CAVERN

It becomes clear that the above analytical method is useful for the estimation of the strain around a tunnel. Therefore, using this method, the

dynamic stress and the acceleration around the large cavern during the strong earthquake is estimated. The N-S component of the El Centro earthquake (1940) is used for an incident motion and its maximum value is set to 50.0 gal considering the design seismic load. A large cavern of a cylindrical shape with the diameter 30.0 m is considered. The surrounding rock ground is an infinite elastic medium whose properties are the same values as the fresh rock in Kikuma. Figure 11 shows the maximum dynamic stress in the circumferential direction (σ_θ) and the maximum acceleration in the horizontal direction. The maximum stress value around the cavern is about 120 t/m^2 in the directions whose angle from the incident wave are 45° and 135°. The maximum acceleration values are almost equal for all the positions. Therefore, the existence of the cavern of this scale does not have much influence on the earthquake motion in the fresh rock.

CONCLUSIONS

This paper presents the dynamic characteristics of the rock ground using the observed earthquake records and the deformation of the service tunnel during earthquakes. Also, the simulation analysis of the strain records is carried out using the analytical method by Mow and Mente. The results obtained in this study can be summarized as follows:

1. The existence of the underground crude oil storage cavern of this scale does not have much influence on the earthquake motion in the rock ground.

2. The maximum acceleration values of the observed earthquakes change only a little in the fresh rock. However, these motions are amplified drastically as they approach the weathered stratum near the ground surface. Hence, the underground oil storage tank in the fresh rock is recognized to have an advantage against earthquakes over the conventional type oil tanks located above the ground surface.

3. The deformation of the service tunnel during earthquakes seems to consist of various modes. However, in approximation, it can be decomposed into two dominant modes which are the uniform expansion and contraction type mode in the vertical direction and the shearing type mode in the horizontal direction.

4. The analytical method used here well simulates the observed strain records. Therefore, using this simple method, the dynamic stress around the storage cavern during earthquakes can be estimated in the design stage.

ACKNOWLEDGMENT

The authors would like to thank Japan National Oil Corporation for permitting to use their observed earthquake records.

REFERENCES

1. Kato, M., "On Performance Test of the First Pilot Plant in Japan for Underground Stockpiling of Crude Oil," Journal of Japan Petroleum Institute, Vol.27, No.3, 179-187, (1984).
2. Miyashita, K., Aoki, k., Hanamura, T. and Kashiwagi, N., "An Investigation of Geomechanics and Hydraulics around an Underground Crude Oil Storage Cavern," International Symposium on Field Measurements in Geomechanics, 1117-1126, (1983).
3. Mow, C. C. and Mente, L. J., "Dynamic Stresses and Displacements Around Cylindrical Discontinuities Due to Plane Harmonic Shear Waves," Journal of Applied Mechanics, December, 598-604, (1963).

Fig. 1 Location of the Demonstration Plant

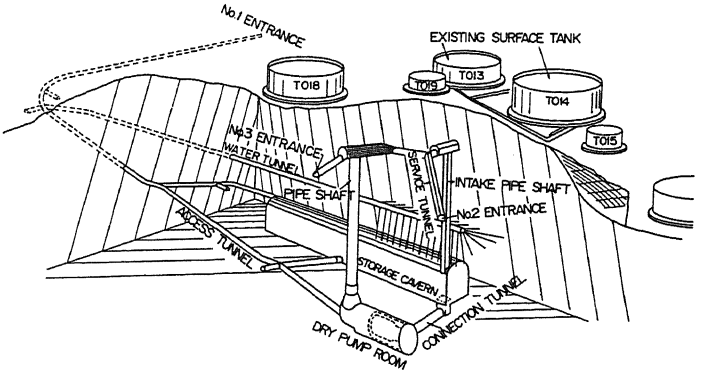

Fig. 2 Perspective View of Kikuma Demonstration Plant

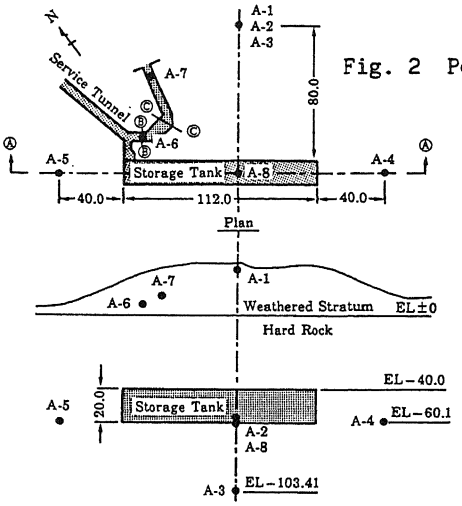

Fig. 3 Location of the accelerometers

Table 1 Result of the Elastic Wave Exploration

Elevation (m)	Vp (km/s)	Vs (km/s)	Poisson's Ratio
+26.70 ~ ±0.0	—	—	—
±0.0 ~ -4.98	2.2	1.0	0.37
-4.98 ~ -48.98	5.0	2.6	0.31
-48.98 ~ -100.98	5.2	2.8	0.30

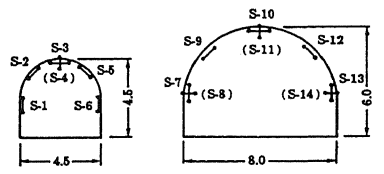

Fig. 4 Location of the Strain Gauges

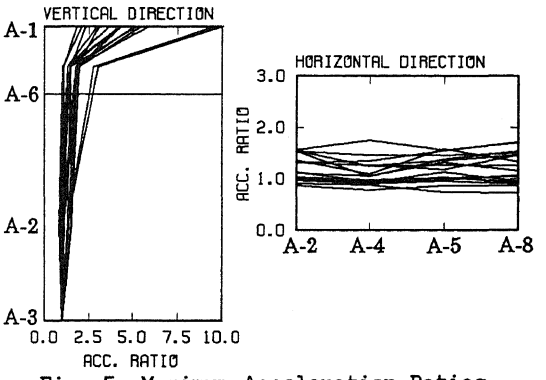

Fig. 5 Maximum Acceleration Ratios

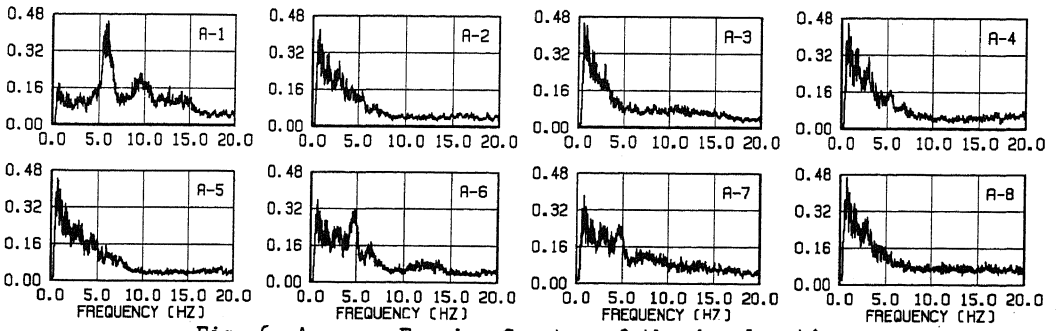

Fig. 6 Average Fourier Spectra of the Acceleration

Table 2 Maximum Strain Values (μ)

No.	S−1	S−2	S−3	S−4	S−5	S−6	S−7
21	0.083	0.073	0.069	0.025	0.098	0.057	0.120
22	0.069	0.176	0.070	0.020	0.156	0.068	0.121
25	0.047	0.043	0.024	0.011	0.040	0.034	0.057
26	0.087	0.068	0.042	0.034	0.067	0.055	0.114
30	0.074	0.058	0.030	0.023	0.076	0.046	0.103
31	0.167	0.276	0.103	0.040	0.231	0.127	0.274

No.	S−8	S−9	S−10	S−11	S−12	S−13	S−14
21	0.018	0.365	0.073	0.029	0.142	0.115	0.021
22	0.027	0.275	0.069	0.035	0.128	0.098	0.020
25	0.010	0.077	0.035	0.009	0.048	0.051	0.005
26	0.020	0.141	0.060	0.029	0.109	0.082	0.025
30	0.017	0.129	0.062	0.023	0.140	0.060	0.019
31	0.051	0.478	0.126	0.055	0.254	0.212	0.069

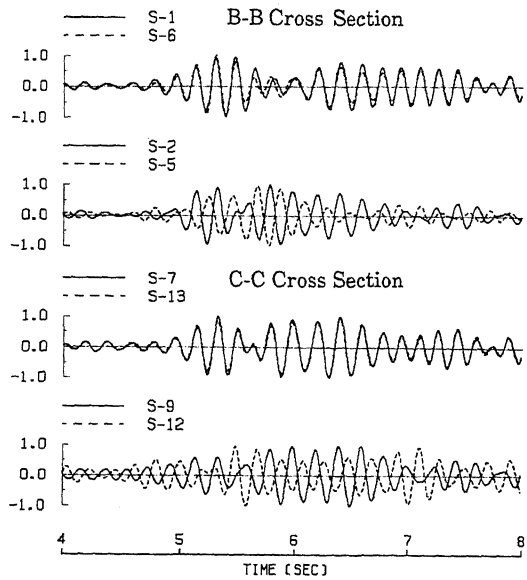

Fig. 8 Principal Motions of the Strain Records

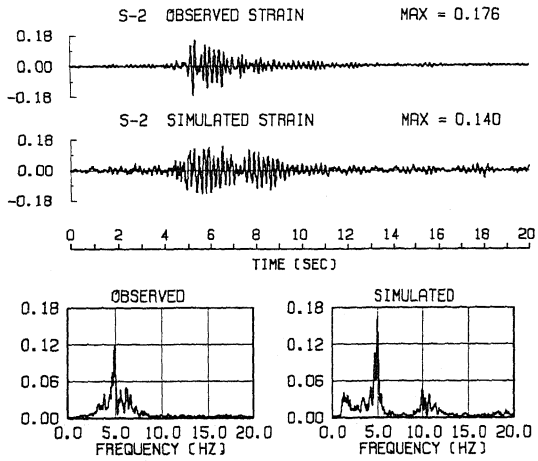

Fig. 10 Results of the Simulation

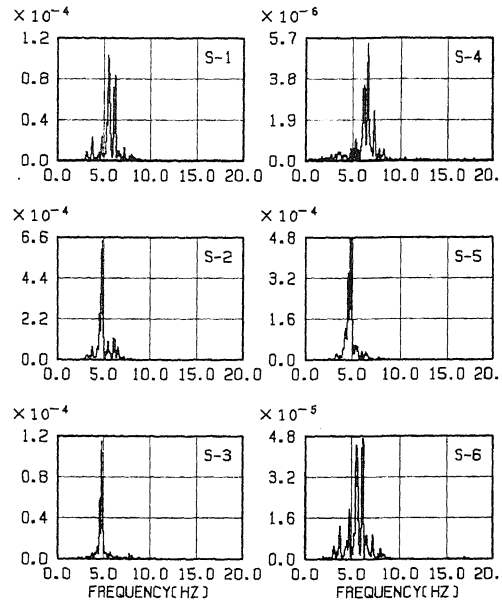

Fig. 7 Power Spectra of the Strain

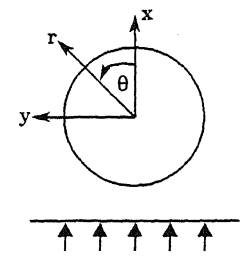

Fig. 9 Analytical Model

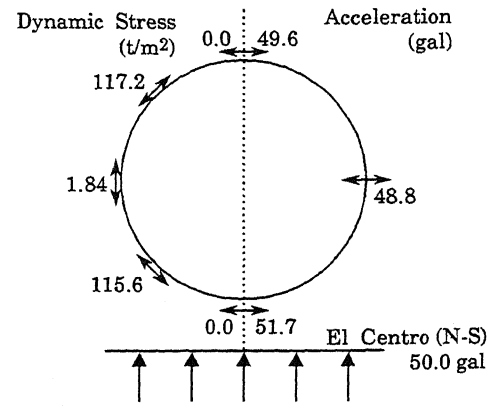

Fig. 11 Dynamic Stress and Acceleration